EGTRIB Journal
JOURNAL OF
THE EGYPTIAN SOCIETY OF TRIBOLOGY
VOLUME 17, No. 3, July 2020, pp. 37 - 47 **ISSN 2090 - 5882**
(Received May 15. 2020, Accepted in final form June 20. 2020) **www.egtribjournal.com**

DYNAMIC CHARACTERISTICS STUDY OF RE-ENTRANT HONEYCOMB AUXETIC STRUCTURE FOR AL6082

M. Elsamanty[1,2], A. Mostafa[1], A. Ibrahim[1]

[1] Benha University, Faculty of Engineering at Shoubra, Mechanical Department, Egypt
[2] Nile University, Smart Engineering Systems Research Center (SESC), Egypt

ABSTRACT
The Auxetic structures were developed to be used in various applications. Regarding the wide spreading of these structures, different research has been developed to study the different static and dynamic characteristics. This paper presents the numerical investigation results of the dynamic characteristics for a re-entrant honeycomb Auxetic Structure based on its Geometrical parameters. The part of the Auxetic system is chosen to be Aluminium. The study begins by constructing the model of the finite element to simulate the structure in the static, transient and modal analyses. These analyses were performed and determined the impact of geometric parameters change on the negative Poisson's ratio, Natural frequency, Damping Ratio of the re - entrant structures.

KEYWORDS
Auxetic Structure, Negative Poisson's Ratio, Re-Entrant Structure, Re-entrant Honeycomb, Dynamic Characteristics, Transient Response, Modal Analysis.

INTRODUCTION
In the automotive, aerospace and construction sectors, many different engineering industries require that their components be lightweight and highly elastic to stand up to operational conditions rather than breakup. The designers have therefore turned to cellular structures. Researchers have been trying over decades to find many kinds of cellular materials that give us unique mechanical properties. One of these is the negative ratio structure of Poisson, also called Auxetic material. As Auxetic materials are extended in one direction, they stretch transverse to the direction of loading. Therefore, if the load is switched from extending to compression, the materials contract in a transversal direction. R. in 1987. Lakes started research with traditional open-cell polymer low-density foams with a Poisson 0.4 ratio, which he could then transform to a reusable structure by allowing each cell's ribs to proliferate permanently inward. The new structure had a negative ratio of -0.7 for Poisson. Negative Poisson foams have been shown to be more robust than traditional foams. Lakes projected that new designs could be used for robust material and air filters resisting shocks, [1].

The re-entrant, [1, 2, 3] honeycomb structure and the structure of rotating squares, [4, 5, 6, 7] are the most common geometries used to build structures with a negative Poisson

ratio. Another common structure with negative Poisson ratio is that R had studied chiral geometry. Lakes, [8, 9]. Lakes Due to the unique properties of the Auxetic structures, many scientists have been interested in studying them and trying to use them in applications. Auxetic structures have good shear characteristics, [10], good resistance to indentation, [11] and good resistance to fracture [12]. In [13, 14, 15] the dynamic characteristics of the Auxetic structures were studied. The Auxetic foam is superior to conventional foam in terms of damping and acoustic properties. Auxetic foams may have a better sound absorption capacity at all frequency levels than conventional foams, [14]. Low volume modules are available to the Auxetic structures, making them more sensitive to hydrostatic pressure and allowing the use of the Auxetic materials in hydrophone design, force sensors and other sensors [16, 17]. The use of these structures as nails is also suggested, [18, 19]. They are also applicable in biomedicine, [20] and in sports applications, [21].

The objective of this research is to study the effect of changes the dynamic characteristics of some engineering parameters of re-entrant Auxetic structure cells. This can help designers to achieve an optimal design for this shape which serves their applications in several applications. There are three sections in this paper. The design of Auxetic structures by means of CAD software. Numerical analysis was then performed via the software ANSYS. Finally, a complete investigation has been accomplished between the length and height for the model with respect to the modulus of elasticity, Negative Poisson's Ratio, Mode shapes and the damping ratio.

Re-entrant Auxetic Model

The specimens in this work were designed with SOLIDWORKS software as illustrated in Fig. 1. The unit cell of the principal structure is re-entrant honeycomb cell. The principal dimensions of this form are also as follows; l is the original cell wall length and h is the vertical walls' height. Where, Ø is the initial angle of the sloping wall to the X axis. T is the thickness of the cell wall. The Auxetic structure thickness is 5 mm. L is the specimen length. H is the specimen height. The number of the cells is symbolized by N.

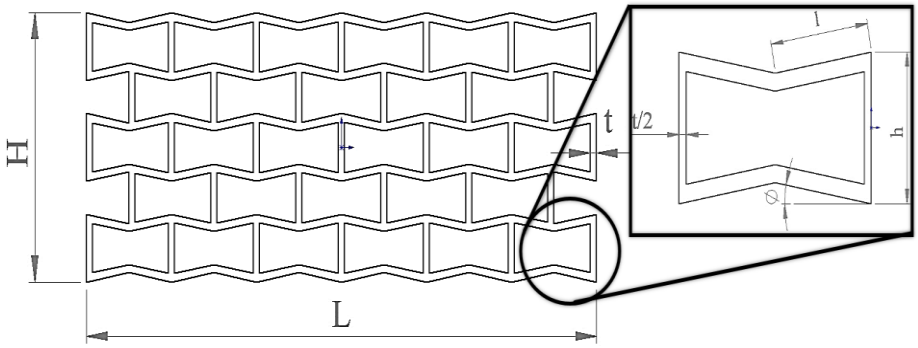

Fig. 1 Re-entrant honeycomb cell.

The parameters chosen to study the effects of their iteration on the structure's dynamic properties were the specimen length L and height H. The Length 'L' values vary from 139 mm, 162 mm to 185 mm. The values of Height 'H' are altering with 58, 68 and 79 mm. The thickness 't' values are changing to 2 mm, 2.2 mm, 2.4 mm, 2.6 mm. The angle values

change from 2º, 4º, 6º, 8º, 10º, 12º to 14º as the cell numbers are varying 4, 5, 6, 7, and 8. A sample of specimens is presented in the following Table 1. The dimensions of the length are defined by the following equation in such a way that the angle value with the length of the inclined cell walls is no longer than the total length of the prescribed limit.

$$L = 2 * N * l * \cos \emptyset \quad (1)$$

Finite Element Analysis

This study uses the software package ANSYS to simulate the behaviour of the tested samples for finite element analysis. Ansys offers the ability to carry out a number of structural analysis (for example static structural analysis, modal analysis, transient analysis, harmonic response analysis, rigid dynamics, etc...). This work included three tests: static structure analysis, modal analysis and transient analysis. Every analysis is divided into several steps: pre-process, method and post-process.

Table 1 Samples of various lengths

Sample No.	h (mm)	l (mm)	T (mm)	N (cells)	Phi (degree)	L (mm)
1	18	17.396	2	4	2	139.09
2	18	17.428	2	4	4	139.09
3	18	17.482	2	4	6	139.09
8	18	20.297	2	4	2	162.28
9	18	20.334	2	4	4	162.28
10	18	20.396	2	4	6	162.28
15	18	23.196	2	4	2	185.46
16	18	23.239	2	4	4	185.46
17	18	23.31	2	4	6	185.46

In the pre-process phase, the CAD model was inserted and material properties, meshing type and size, fixation method and loading method were chosen. Moreover, the material for this study is Aluminum (Al 6082). The material properties are tested by means of a tension test and the obtained values are shown in Table 3.

Table 2 Al 6082 mechanical characteristics

Material	E (MPa)	υ	σ_{Ult} (MPa)	σ_Y Yield(MPa)	ρ (kg\ m^3)
Al 6082	69000	0.33	140	85	2710

Table 3 meshing size

Min. Size	Proximity Min Size	Max Face Size	Max Size	Growth Rate	Minimum Edge Length	Nodes	Elements
1.0 mm	1.0 mm	2.0 mm	2.0 mm	Default (1.850)	5.0 mm	66227	10320

In order to achieve the best possible result, and to rely on these tests the best mesh size as demonstrated in Table 3. Meshing was tested at different sizes and shape to reach the optimal size and shape. Five iterations of meshing were performed and compared to each other. Table 3 presents the best mesh size that make the final results are achieved with error 5% compared to the smallest meshing size. The meshing shape was iterated to reach the Hexahedral shape as presented in Fig. 2. The specimen was fixed on one end, and the other end was free as cantilever beam as shown in Fig. 3.

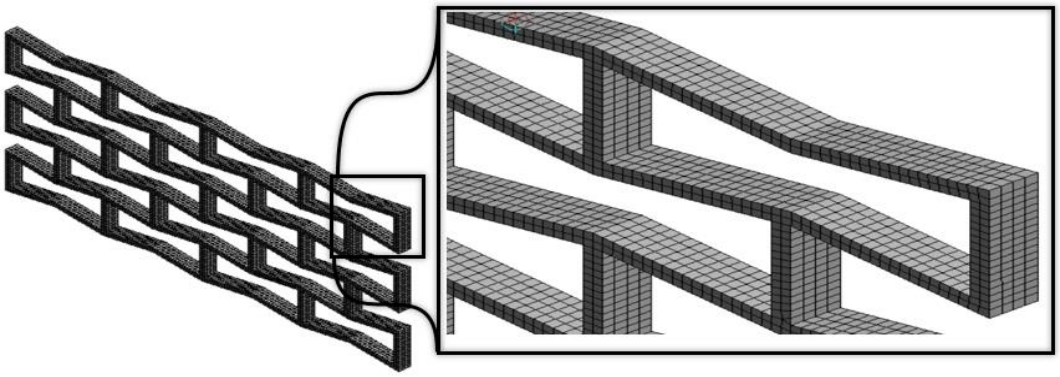

Fig. 2 Meshing size and Shape.

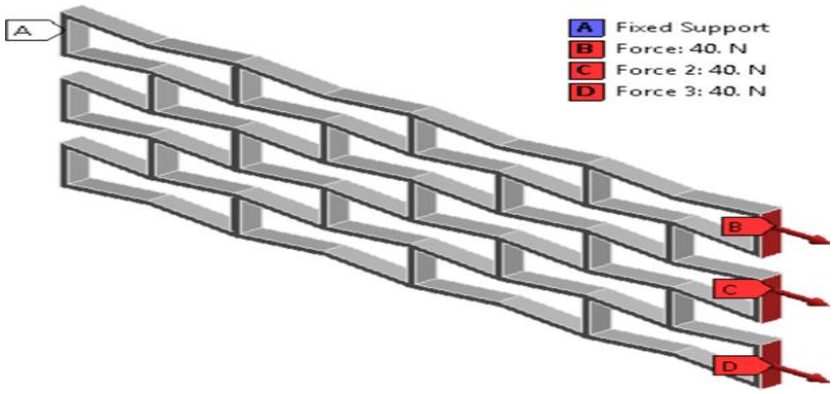

Fig. 3 The load applied to the sample.

In the second process phase, three tests were applied in this project, as mentioned above: static structure analysis, modal analysis and transient analysis. The static structure analysis was used for determining the load effects on structures. Moreover, this test is used to calculate the deformations, stresses and strain, then determining the impact on Young's modulus and Poisson 's ratio of adjusting the chosen model parameters. For a linear static structural analysis, the displacements {x} are solved for in the matrix equation (2). Where [K] is the stiffness matrix and {F} is the applied force.

$$[K]\{X\} = \{F\} \quad (2)$$

The modal analysis test is used to calculate re-entrant honeycomb Auxetic structure natural frequencies. The equation of motion of free vibration for mechanical system can expressed as follow, Where [M] and [K] mass and stiffness matrices.

$$[M][\ddot{x}] + [C][\dot{x}] + [K][x] = 0 \quad (3)$$

The natural frequency can be obtained by Equation

$$\left|([K] - \omega_n^2\ [M])\right| = 0 \quad (4)$$

In ANSYS, there are several mode-extraction methods; Block lanczos, PCG lanczos, unsymmetric and supernode. Block lanczos is used in this work to get mode shapes. The last step is the post- process which compile all the analysis results and the effects of changing model parameters on the dynamic characteristics.

Finite Element Results

Figure 4 presents the result of the static structure analysis of the Auxetic honeycomb structure under tension test. The presented data for the specimen sample with L=139.09 mm, Ø=2º, N=4 and cell length l=17.396 mm. So, it can be noticed that the specimen under ension increases in length and width which confirms the behavior of the Auxetic structure which results in confirmation of the ratio of the negative Poisson. The rate of increase in length and width was 4.3% and 7.2% respectively. Moreover, the modal analysis results are presented in Fig. 5A, 5B. The first mode and third modes are for the bending around Y and Z axis. The natural frequency for these two modes were 129.25, 345.07 Hz for the first and third modes. These low frequencies could help in improving this structure to be used as a damping structure. The transient analysis results are presented in Fig. 6A, 6B, the Auxetic structure tend to damping the free oscillation in 0.6 Seconds.

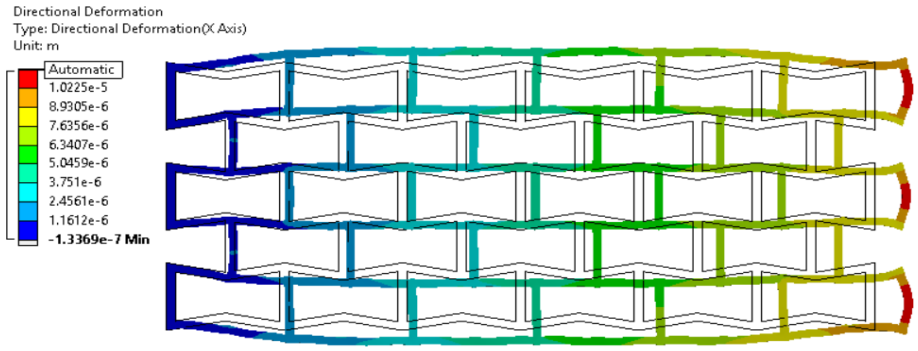

Fig. 4 behavior of sample under tension.

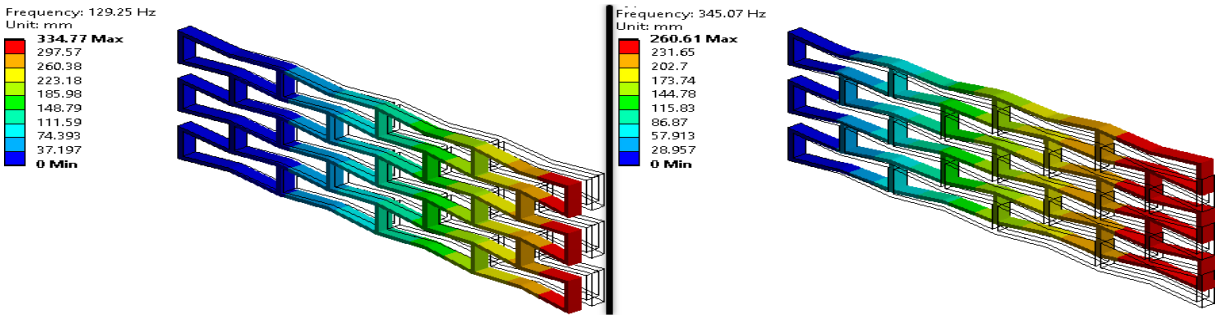

(A) (B)

Fig. 5 The natural Frequency modes, (A) 1st mode shape (First bending about Y axis) and (B) 3rd mode shape (First bending about Z axis).

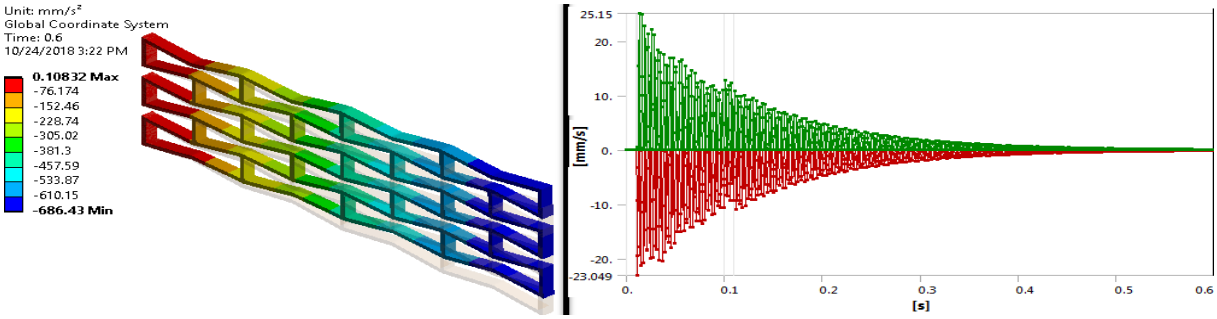

(A) **(B)**

Fig. 6 (A) Transient analysis (B) Time response in transient analysis.

RESULTS AND DISCUSSION

The results from ANSYS have been gathered and collected together to study the effect of the specimen geometrical parameters on the static, modal and transient response. These results have been categorized based on the change of the Height and Length of specimen with respect to Young's Modulus and Poisson's ratio in the static mode. Then, the same parameters will be presented with respect to the change of natural frequencies. Finally, L and H will be studied with respect to the damping ration. All these results will be presented at constant of N 'Number of Cells' and Ø 'Cell angle'.

Effect of Height and Length at Static Conditions

The effect of increasing the specimen height at constant length of 139mm leads to decrease the Young's Modulus as presented in Fig. 7. The rate of change was noticed as 4.1% with respect to the young's Modulus of the base material. Moreover, the increase of the specimen height leads to decrease the value of the Poisson's ratio as presented in Fig. 8. This decrease was rated as 5.55% with respect to the smallest height.

On the other hand, the increase of the specimen length at constant Height of 58.6 mm leads to a very small change in modulus of elasticity by 0.35%. Furthermore, the increase in the same length leads to increase the negative Poisson's ratio by 16.6%. These notice are important regarding that the base material Young's modulus remains approximately constant with a significant change in the Poisson's ratio correlated to the change in the geometrical parameters as shown in Fig. 9 and 10.

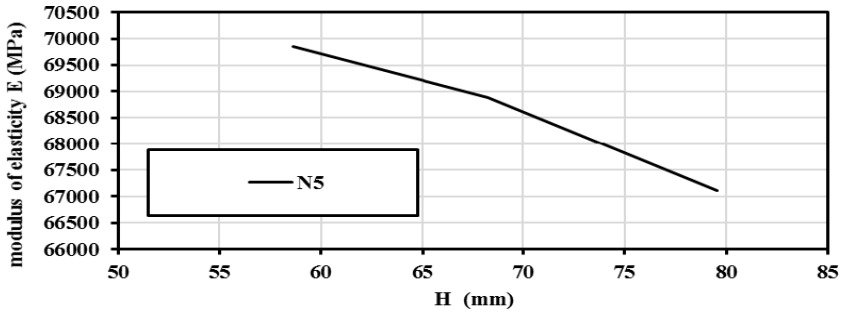

Fig. 7 Specimen Height 'H' effect on Young's modulus at constant rib angle Ø = 2º.

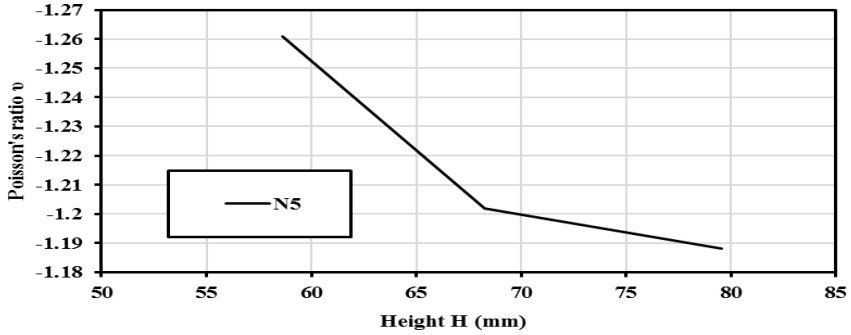

Fig. 8 Specimen Height 'H' effect on Poisson's ratio at constant rib angle Ø = 2º.

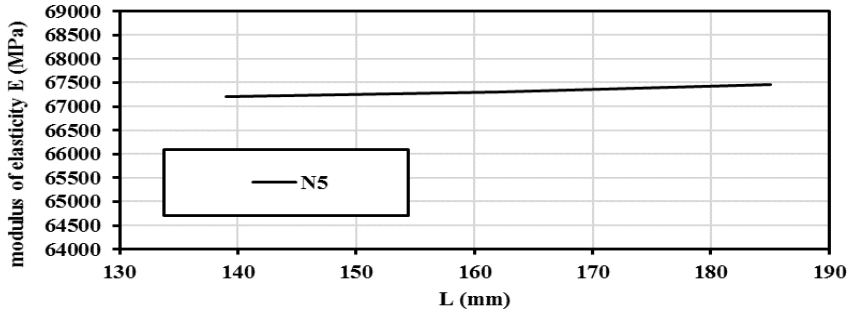

Fig. 9 Specimen Length 'L' effect on Young's modulus at constant rib angle Ø = 2º.

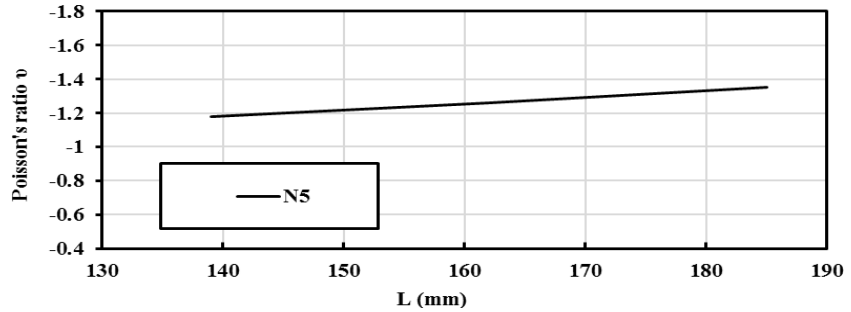

Fig. 10 Specimen Length 'L' effect on Poisson's ratio at constant rib angle Ø = 2º.

Effect of Height and Length on Modal Analysis

The effect of shape height on natural frequencies of the first and third mode is studied. For samples with the same length L, thickness T and angle of rib. The first natural frequency increases when the sample height increases. With the change from 58 mm to 79 mm in the total value of H, the first natural frequency was increased by 65 % as shown in Fig. 11. But, the rate of increase decreased with the increase in the cell count (N) and its value reached 59% in N=8 cells. Moreover, an increase of 51% of the 3rd Natural Frequency from 341,9 Hz to 519,1 Hz as shown in Fig. 12. But, this rate of increase decreases with an increase in cell count (N) and its value reaches N=8 cells by 39%. The overall increase in specimen height increases sample inertia, leading to an increase in rigidity and natural frequency.

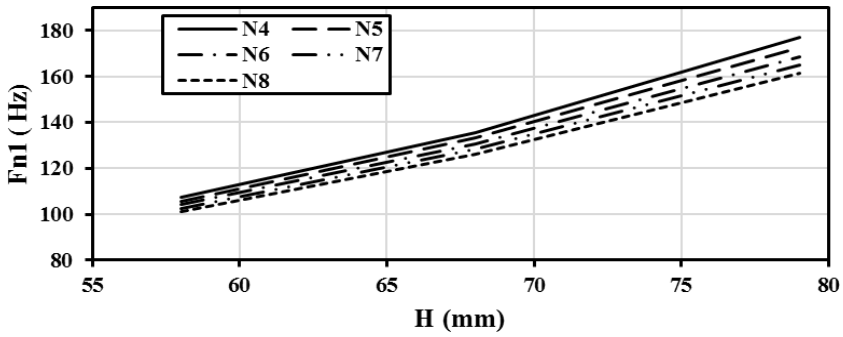

Fig. 11 Specimen Height 'H' effect on First Mode Natural Frequency Fn_1. at constant rib angle Ø = 2º.

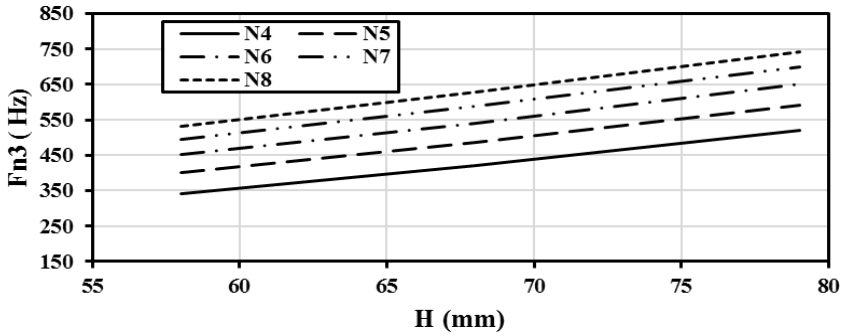

Fig. 12 Specimen Height 'H' effect on Third Mode Natural Frequency Fn_3 at constant rib angle Ø = 2º.

On the other contrary, the effects of the shape length on natural frequency mode 1 and 3 are investigated. When the sample length increases, as shown in Fig. 13 and Fig. 14, the first and third natural frequency mode decreases. The change in value of the total length L from 139 mm to 185 mm led to a decrease of 40% in the first natural frequency, a decrease almost constant in the number of cells. Increased length leads to a reduction in rigidity, leading to a decrease in the natural frequency.

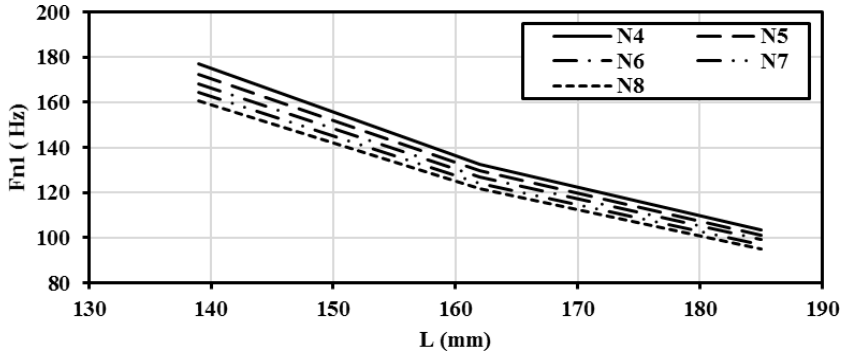

Fig. 13 Specimen Length 'L' effect on First Mode Natural Frequency Fn_1 at constant rib angle Ø = 2º.

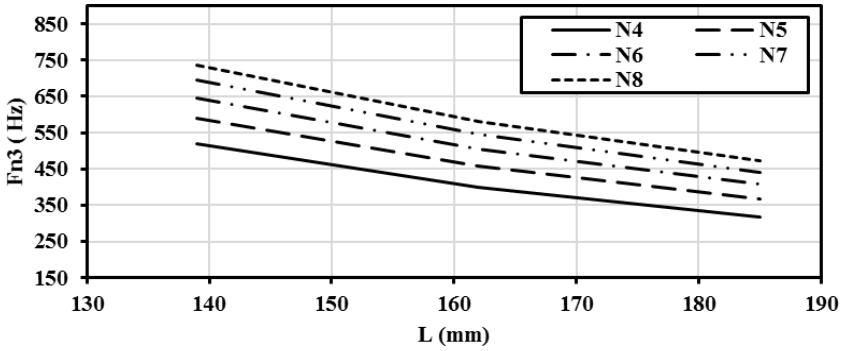

Fig. 14 Specimen Length 'L' effect on Third Mode Natural Frequency Fn_3 at constant rib angle Ø = 2º.

Effect of Height and Length on Damping Ratio

For specimens with the same rib thickness T and rib angle Ø, the damping ratio is increased at the number of cells N = 4 cells as the specimen height increases. The change of the value of total height H of 58 mm to 79 mm resulted in an increase of 50% in the damping ratio. But this rate of increase decreases with increases in the number of cells (N) and its value at N=8 as shown in Fig.15 reaches 26%. In contrast, as shown in Fig.16, the damping ratio decreases when the sample length increases. At N=4 cells, the increase from the length of 139mm to 185mm leads to a 36 percent decrease in the damping ratio from 0.331 to 0.211. This rate decreases as the number of cells increases and reaches N = 8 cells by 29%.

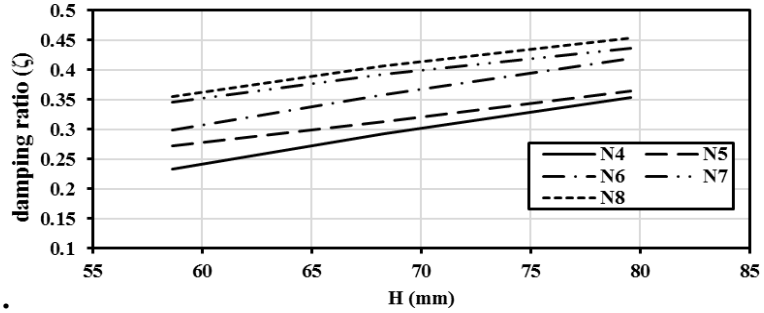

Fig. 15 Specimen Height 'H' effect on damping ratio ζ at constant rib angle Ø =2º.

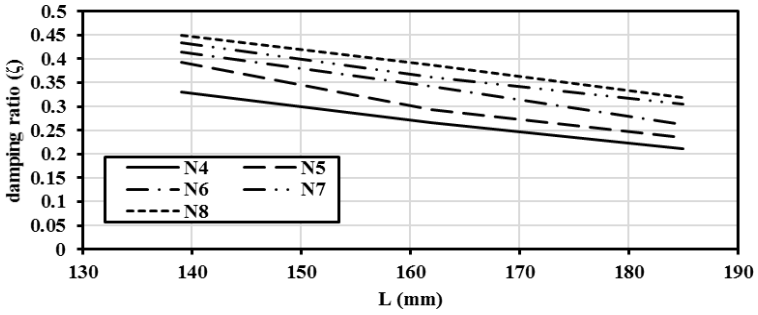

Fig. 16 Specimen Length 'L' effect on damping ratio ζ at constant rib angle Ø =2º.

CONCLUSIONS

Several important conclusions can be extracted that could help the designers to select the appropriate re-entrant Auxetic honeycomb structure to prevent resonance cases and reduce any unwanted vibrations. It is concluded that the increase of height reduces the elastic modulus and negative structural ratio of Poisson, but also increases the fundamental natural frequencies and structural damping ratio. The length increase increases the negative Poisson ratio with a small effect on elastic modules, but reduces the basic natural frequencies and structure damping ratio.

REFERENCES

1. Lakes, R., "Foam Structures with a Negative Poisson's Ratio", *Science. 235*, pp. 1038–1040 (1987).

2. Liu, Y. and Hu, H., "A review on Auxetic structures and polymeric materials", *Sci. Res. Essays 5*, pp. 1052–1063 (2010).

3. Grima, J. N., Cauchi, R., Gatt, R. and Attard, D., "Honeycomb composites with Auxetic out-of-plane characteristics", *Compos. Struct.* 106, pp. 150–159 (2013).

4. Grima, J. N. and EVANS, K. E., "Auxetic behaviour from rotating squares", *J. Mater. Sci. Lett. 19*, pp. 1563 – 1565 (2000).

5. Grim, J. N., Jackson, R., Alderson, A. and Evans, K. E., "Do Zeolites Have Negative Poisson's Ratios", *Adv. Mater.* pp. 1912–1918 (2000).

6. Grima, J. N., Alderson, A. and Evans, K. E., "Negative Poisson's Ratios from Rotating Rectangles", *Comput. METHODS Sci. Technol. 10*, pp. 137–145 (2004).

7. Grima, J. N., MANICARO, E. and ATTARD, D., "Auxetic behaviour from connected different-sized squares and rectangles", *Proc. R. Soc. A 467*, pp. 439–458 (2011).

8. Lakes, R., "Deformation mechanisms in negative Poisson's ratio materials: structural aspects", *J. Mater. Sci. 26*, pp. 2287–2292 (1991).

9. Prall, D. and Lakes, R. S., "Properties of a Chiral Honeycomb with a Poisson's Ratio", *Int. J. Mech. Sci. 39*, pp. 305 314 (1997).

10. Yang, W., Li, Z. M. Shi, W., XIE, B.-H. aand YANG, M.-B, "Review On Auxetic materials" *J. Mater. Sci. 39*, pp. 3269 – 3279 (2004).

11. Krishna, B., Saxena, K., Das, R. and Calius, E. P., "Three Decades of Auxetic Research À Materials with Negative Poisson's Ratio: A Review", *Adv. Eng. Mater.* pp. 1–24 (2016).

12. Science, O. and City, I., "Fracture toughness of re-entrant foam materials with a negative Poisson's ratio: experiment and analysis". *Int. J. Fract.* pp. 73–83 (1996).

13. Matteo Bianchi and Fabrizio Scarpa., "Vibration transmissibility and damping behaviour for Auxetic and conventional foams under linear and nonlinear regime", *Smart Mater. Struct*, pp. 1–16 (2013).

14. F Scarpa, L. G. C. and J. R. Y., "Dynamic properties of high structural integrity Auxetic open cell foam", *SMART Mater. Struct. 13*, pp. 49–56 (2004).

15. Essassi, K., Rebiere, J., Mahi, A. E. L., Amine, M. and Souf, B., "Experimental and numerical analysis of the dynamic behavior of a bio-based sandwich with an Auxetic core", *J. Sandw. Struct. Mater.* pp. 1–20 (2019).

16. Avellaneda, M. and Swart, P. J., "Calculating the performance of 1 – 3 piezoelectric composites for hydrophone applications: An effective medium approach", *Acoust. Soc. Am. 103*, pp. 1449–1467 (2014).

17. J., Bhullar, S., Lee, P. C. and Jun, M. B. G., "Design and fabrication of Auxetic stretchable force sensor for hand rehabilitation", *Smart Mater. Struct.* pp. 1–8 (2015).

18. Choi, J. B. and Lakes, R. S., "Design of a fastener based on negative Poisson's ratio foam", *Cell. Polym. 10,* pp. 205–212 (1991).
19. Ren, X., Shen, J., Tran, P., Ngo, T. D. and Xie, Y. M., "Auxetic nail: Design and experimental study", *Compos. Struct.* pp. 184, 288–298 (2018).
20. Liu Q., "Literature Review: Materials with Negative Poisson's Ratios and Potential Applications to Aerospace and Defense", *Defense Science and Technology,* (2006)
21. Sanami M., Ravirala N., Alderson K., and Alderson A., "Auxetic materials for sports applications", Procedia Eng., Vol. 72, pp. 453 - 458, (2014).